
Article:
Sun, J., Li, P. and Susmel, L. orcid.org/0000-0001-7753-9176 (2022) Acceleration factor and experimental validation of aluminum alloy under narrow-band random excitation. Fatigue and Fracture of Engineering Materials and Structures. ISSN 8756-758X

https://doi.org/10.1111/ffe.13916

Acceleration factor and experimental validation of aluminum alloy under narrow-band random excitation

Jiachen Sun [a], Piao Li [a, b†], Luca Susmel [b]

[a] *College of Aerospace Engineering, Nanjing University of Aeronautics and Astronautics, Nanjing 210016, China*

[b] *Department of Civil and Structural Engineering, The University of Sheffield, Sheffield S1 3JD, UK*

Abstract

In order to reduce the vibration fatigue test time of aeronautical engineering components made of aluminum-alloy, a random vibration fatigue acceleration model under narrow-band excitation is proposed in this paper. A three-parameter *S-N* curve is adopted to consider the effect of small stress response, while a scale factor α is introduced to consider the effect of stress distribution. The random vibration fatigue tests of 2024-T3 and 7075-T6 aluminum-alloy specimens with elliptical holes are performed, where the vibration fatigue lives of load spectra with the same bandwidth and different excitation acceleration levels are obtained. The test results show that the proposed model is in sound agreement with the test results.

Key words: Random vibration; Acceleration factor; Three-parameter *S-N* curve; Root mean square of stress

1. Introduction

Vibration fatigue is a problem that seriously endangers the reliability and safety of important engineering components and structures. In this context, vibration fatigue tests always require a high economical and time cost, so the application of accelerated vibration fatigue test is one of the important aspects in the design against fatigue process.

Accelerated vibration fatigue test refers to the reduction of vibration fatigue test life by increasing the magnitude of the random vibration excitation [1]. The ratio between vibration fatigue life before and after acceleration is termed acceleration factor γ. Different acceleration analyses and test methods are carried out according to the different excitation spectrums of random vibration being adopted. The amplitude enhancement method is commonly used in the design of vibration fatigue equivalent accelerated test, which is based on an inverse power-law . By keeping the spectral pattern unchanged while the vibration amplitude is increased proportionally at each frequency point, the extent of the cumulative fatigue damage is set to be consistent before and after acceleration so that an equivalent accelerated test is designed effectively[2,3].

The key to the design of vibration accelerated test lies in the estimation of the vibration acceleration factor. It can be calculated by following different strategies and is related to the smoothness and gaussianity of the loading spectrum. In this setting, Allegri and Zhang [3] proposed to use an inverse power law to address stationary broadband Gaussian random processes. The formula of acceleration factor based on the equivalent von Mises stress criterion is given simultaneously, which is widely used in engineering practice. However,

Corresponding author. E-mail address: lipiao@nuaa.edu.cn

by conducing specific validation tests Benasciutti [4] subsequently pointed out the limitations associated with the use the equivalent von Mises stress criterion in the study of vibration acceleration. As far as non-gaussian random processes are concerned, Yu Jiang et al. [5] gave the expression of the relationship between the power spectral density (PSD) of accelerated excitation and the root mean square (RMS) value of stress. Subsequently, the expression of vibration acceleration factor related to the power spectral density of accelerated excitation was obtained, then they adjusted the excitation signal kurtosis to discuss the influence of non-Gaussian distribution on accelerated vibration tests. Zhiwei et al. [6] and Shires [7] studied the solution of the acceleration factor under broadband non-gaussian distribution by introducing the concept of the G_{rms}-N curve. Kim [8] conducted uniaxial accelerated vibration tests under three loading conditions and carried out relevant studies on accelerated vibration tests. Ozsoy et al. [9] calculated the acceleration factor according to the power spectral density of the accelerated excitation spectrum and carried out accelerated vibration tests of aerospace components. Pothula et al. [10] studied the influence of damping on accelerated vibration tests.X. Wu et al.[11] and W. Hu et al. [12] studied the vibration acceleration fatigue of cantilever beam and train gearbox housing respectively. In other relevant studies, equivalent accelerated tests were designed using different strategies, with this being done by looking at the details of the vibration excitation load spectrum [13-18].

Owing to the fact that the vibration fatigue of an aircraft structural component is mainly controlled by the first-order natural frequency response, in the present paper, first the acceleration excitation spectrum is designed and then the analytical model of accelerated test is proposed. Subsequently, the design of vibration fatigue accelerated life tests and the vibration fatigue tests of two kinds of aluminum alloy specimens with elliptical holes are completed.

2. Narrow-band random vibration fatigue accelerated test model

Examination of the state of the art shows that the inverse power law is widely used as acceleration model . This approach adopts the RMS stress as acceleration parameter and uses Basquin’s formula to characterize the fatigue performance of materials. However, it does not reflect the influence of the energy distribution in the frequency domain on the calculation of acceleration factor under the same RMS [19]. Further, it also ignores the contribution to fatigue damage from a large number of small loads in the vibration response.

The three-parameter S-N curve model [20] is adopted in this paper, which can well characterize the fatigue properties of materials in the medium and long fatigue life region, i.e.:

$$(S\text{-}S_{\text{e}})^{b} N = C \tag{1}$$

where S_{e} is the material endurance limit, b and C are material fatigue constants to be determined experimentally.

According to Miner's linear cumulative damage theory, fatigue damage under variable amplitude load can be quantified as follows:

$$D = \sum D_i = \sum \frac{n_i}{N_i} \tag{2}$$

where n_i represents the number of load cycles at the *i-th* stress level, S_i; N_i represents the fatigue life of the structure when the stress level is equal to S_i - which can directly be obtained via Eq. (1) and can be denoted also as $N(S_i)$. For continuously distributed stress states, the number of load cycles within the stress range (S_i, $S_i+\triangle S_i$) is as follows,

$$n_i = \nu T \sum p(S_i)\Delta S_i \tag{3}$$

where ν is the number of stress cycles per unit time, $p(S_i)$ is the probability density distribution function of stress amplitude. By substituting Eq. (3) into Eq. (2), it is straightforward to obtain:

$$\begin{aligned} D &= \nu T \sum \frac{p(S_i)\Delta S_i}{N_i} \\ &= \nu T \int_0^{\infty} \frac{p(S)}{N(S)} \mathrm{d}S \end{aligned} \tag{4}$$

The hypothesis is formed here that stress levels lower than the endurance limit, S_e, give no contribution to the accumulation of fatigue damage. Accordingly, the integral lower limit of Eq. (4) can be replaced by S_e, so that:

$$\begin{aligned} D &= \nu T \int_{S_e}^{\infty} \frac{p(S)}{N(S)} \mathrm{d}S \\ &= \frac{\nu T}{C} \int_{S_e}^{\infty} \left(S - S_e\right)^b \, p(S) \mathrm{d}S \end{aligned} \tag{5}$$

According to the integral theorem, Eq. (5) can be expressed as

$$\begin{aligned} D &= \frac{\nu T}{C} [\left(S - S_e\right)_c]^b \int_{S_e}^{\infty} p(S) \mathrm{d}S \\ &= \frac{\nu T}{C} [\left(S - S_e\right)_c]^b \end{aligned} \tag{6}$$

where $p(S)$ is the probability density function of the stress amplitude; $[(S\text{-}S_e)_c]^b$ is the bth-order moment of S_e because the integral of $p(S)$ is 1. According to the definition of product moment, as shown in Fig. 1, there must be a scale factor α - $\alpha \in (0,1)$ – so that:

$$\left[(S - S_e)_c\right]^b = \left[\alpha (S_{\max} - S_e)\right]^b \tag{7}$$

where $S_{\max}$ is the maximum value of the vibration response stress.

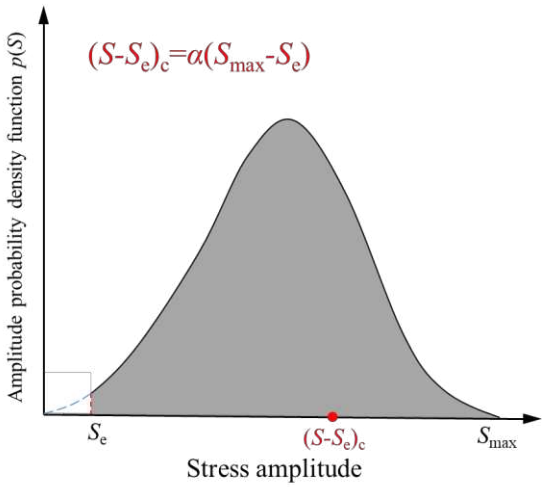

Fig. 1. Schematic diagram of scale factor.

Eq. (6) can be re-written as

$$D = \frac{\nu T}{C}\alpha^b \left(S_{\max} - S_e\right)^b \tag{8}$$

According to Eq. (8), the expressions of the fatigue accumulation damage of the original excitation spectrum, D_0, and the fatigue accumulation damage of the accelerated spectrum, D_A, are as follows, respectively:

$$D_0 = \frac{\nu_0 T_0}{C}\alpha_0^b \left(S_{\max} - S_e\right)^b \tag{9}$$

$$D_A = \frac{\nu_A T_A}{C}\alpha_A^b \left(S_{\max} - S_e\right)^b \tag{10}$$

In a narrow-band random excitation, the number of cycles per unit time ν satisfies the equation $\nu=\nu_p=\nu^+$ [21]. Under the condition of constant bandwidth, only increasing the vibration magnitude in equal proportion will not have a great influence on the number of stress cycles per unit time, so $\nu_0=\nu_A$ can be considered. According to the principle of equal damage (i.e., $D_0=D_A$), the acceleration factor γ can then be obtained as follows:

$$\gamma = \frac{T_0}{T_A} = \left(\frac{\alpha_A}{\alpha_0}\right)^b \tag{11}$$

The scale factor is related to the exponent b of the S-N curve and the probability density function $p(S)$ of the response stress amplitude. Since b is a material constant and is not related to the excitation load, the scale factor α is only related to the excitation spectrum.

3. Experimental design

3.1 Test specimen

The test materials were aluminum alloys 2024-T3 and 7075-T6. The test specimen was a plate with an elliptical hole. A schematic view of the notched specimens together with the relevant dimensions is reported in Fig. 2.

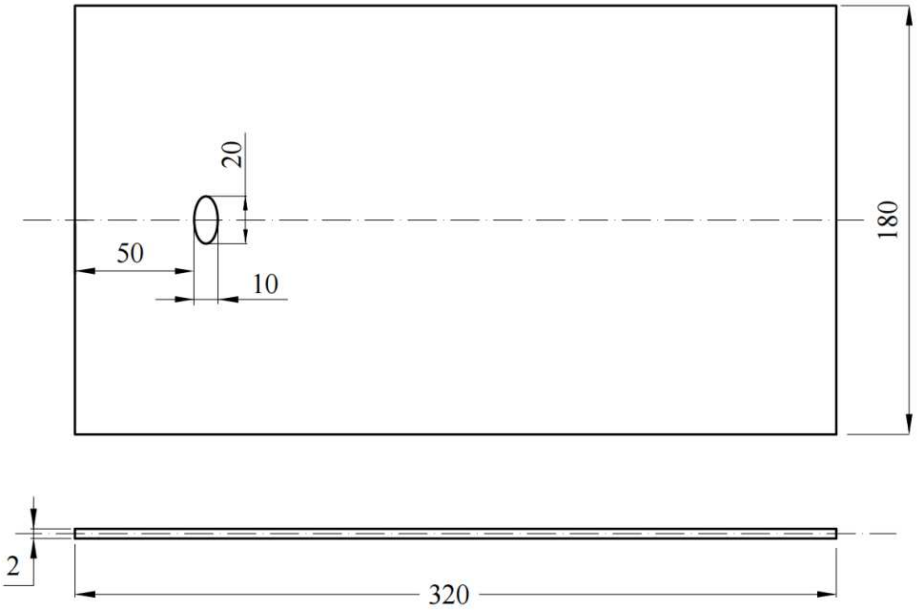

Fig. 2. Dimensions of test specimens for 2024-T3 and 7075-T6.

3.2 Determination of the excitation spectrum

As shown in Fig. 3, one end of the test specimen was fixed and the other end was fitted with a mass stack of 200g. Based on the vibration environment of an aircraft structure, the base vibration excitation level was taken equal to S1-0 and S2-0 as shown in Table 1.

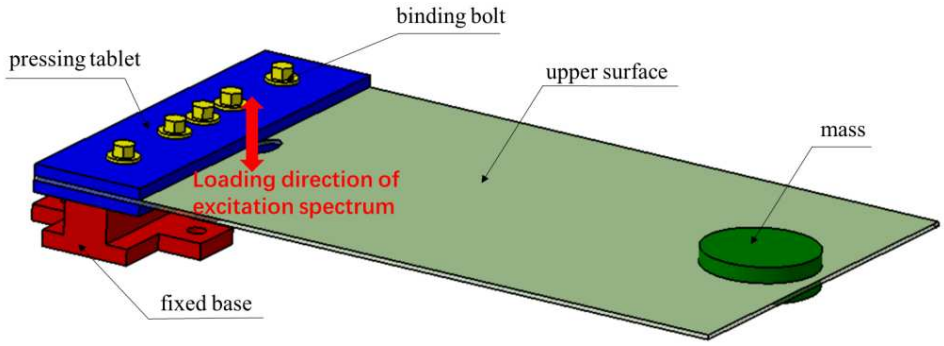

Fig. 3. Installation diagram of specimen in fatigue vibration test.

To calculate the response stress at the critical location and obtain the first-order natural frequency, the test specimen was modelled using the Finite Element Method (FEM). Fig. 4 shows an example of the finite element model of the test piece, which included 38968 hexahedral elements. Fig. 5 shows the boundary condition that were used in the simulations. The six degrees of the edge of the elliptical hole were constrained during the modal analysis.

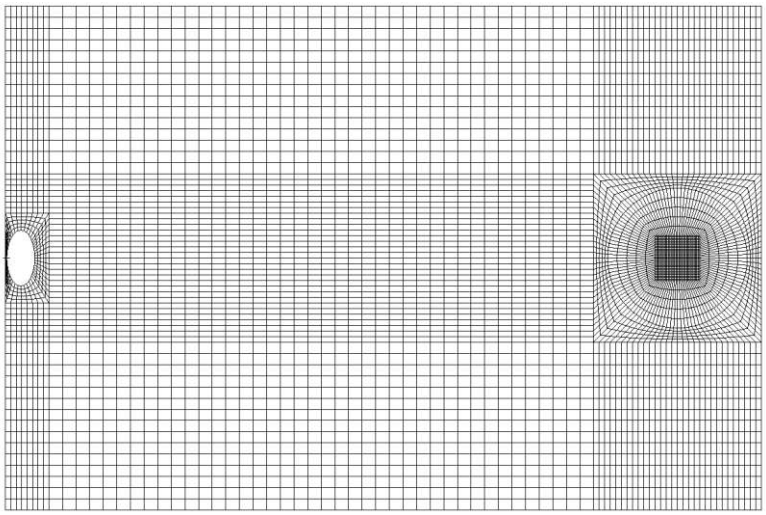

Fig. 4. Finite element model of test specimen.

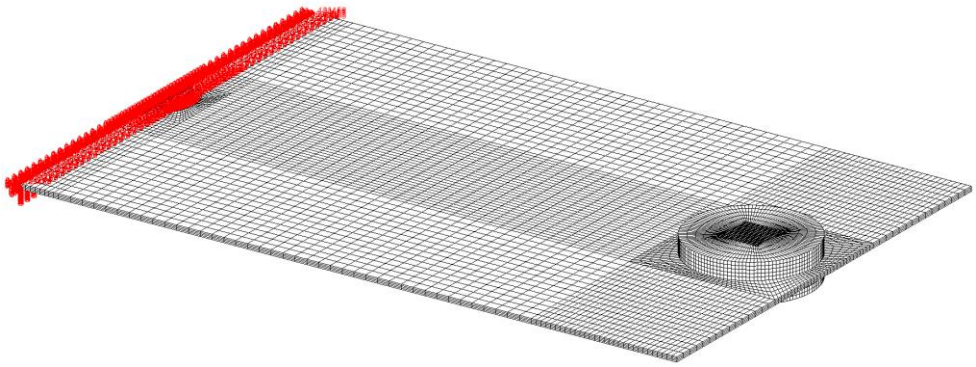

Fig. 5. Boundary condition of test specimen.

According to the results obtained via the FEM, the first-order natural frequency of the 2024-T3 test specimen was 12.74Hz, whereas that of the 7075-T6 test specimen was 12.49Hz.

If one assumes that the excitation spectrum is a narrow-band rectangular spectrum as shown in Fig. 6, then the magnitude must increase as shown in Table 1 when the spectral type of the accelerated excitation spectrum remains unchanged.

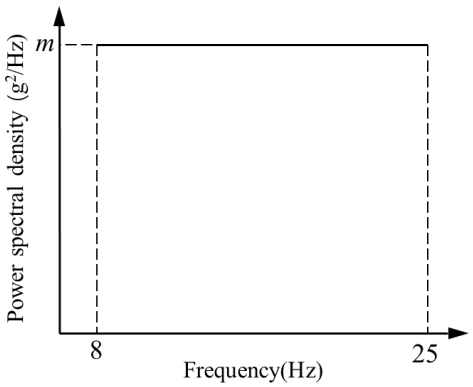

Fig. 6. Load spectrum of accelerated vibration test.

Table 1

Load spectrum parameters of accelerated vibration test.

Material	Excitation spectrum number	Power spectral density magnitude ($g^2 \cdot Hz^{-1}$)
2024-T3	S1-0	0.04
	S1-1	0.10
	S1-2	0.12
	S1-3	0.14
7075-T6	S2-0	0.06
	S2-1	0.18
	S2-2	0.20
	S2-3	0.22

3.3 Acceleration factor estimation

The location of the hot-spot in the test specimen was obtained by the FEM, as shown in the Fig. 7.

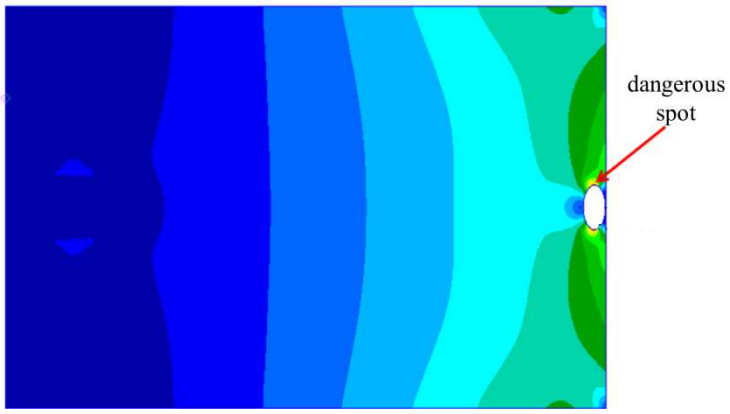

Fig. 7. Dangerous spot of specimen with elliptical hole under vibration environment.

Fig. 8 shows the curves of the response stress spectral density at the critical locations under different load spectra that were obtained numerically (FEM) by random vibration analysis. Fig. 9 shows the probability density function of the stress amplitude which was obtained by fitting with the Dirlik model.

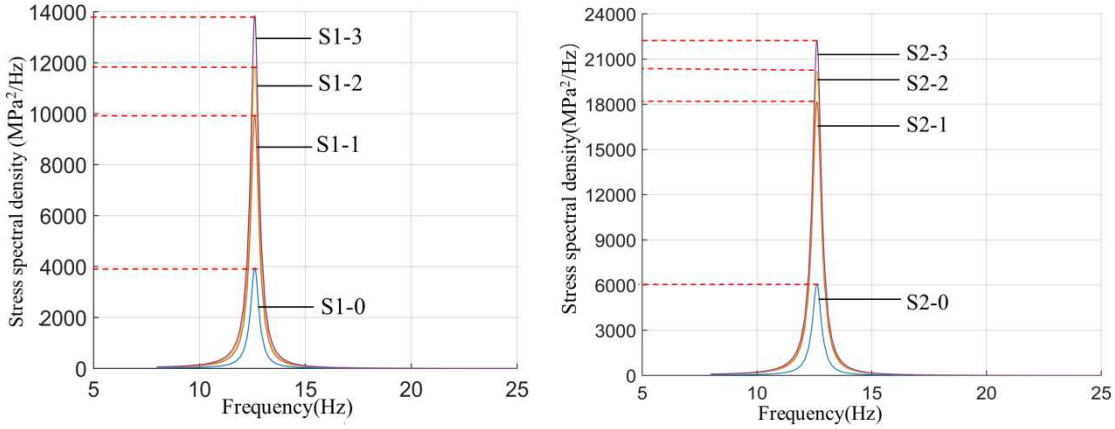

(a) 2024-T3 test specimen (b) 7075-T6 test specimen

Fig. 8. Stress spectrum response at dangerous spots.

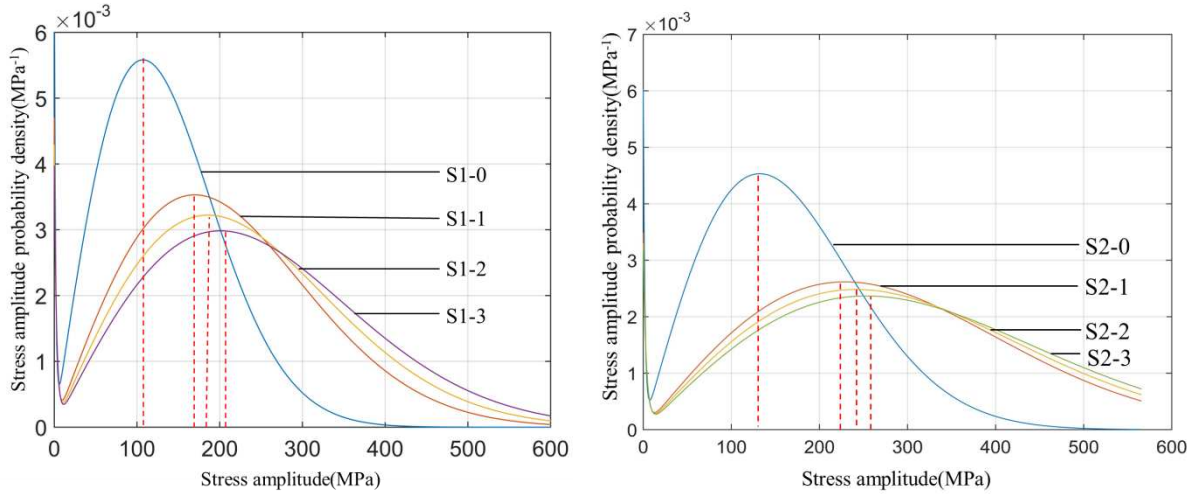

(a) 2024-T3 test specimen (b) 7075-T6 test specimen

Fig. 9. Stress amplitude probability density function.

Fig. 8 shows that increasing the vibration magnitude mainly increases the response magnitude near the resonant frequency, but has little effect on the vibration acceleration in the non-resonant region. Fig. 9 shows that with the increase of the vibration magnitude, the stress corresponding to the peak of the probability density increases gradually: the mode shifts to the right and the shape of the probability density curve tends to be flat.

The three-parameter *S-N* curve formulas [22] of the two kinds of materials used in this paper are:

$$\begin{aligned} &\text{2024-T3:} \quad N_{\mathrm{f}}(S\text{-}74)^{4.0}=10^{13.8} \\ &\text{7075-T6:} \quad N_{\mathrm{f}}(S\text{-}78)^{4.3}=10^{15.1} \end{aligned} \tag{14}$$

The FEM was used to obtain the RMS value of the response stress at the hot-spot under different load spectra within the accelerated test range. The Dirlik model was used to calculate the probability density distribution function of the response stress amplitude, $p(S)$, which was used to calculate the scale factor α under different excitation spectra (see Fig. 10). According to Fig. 10, it can be seen that the scale factor was basically linear with the RMS value of stress.

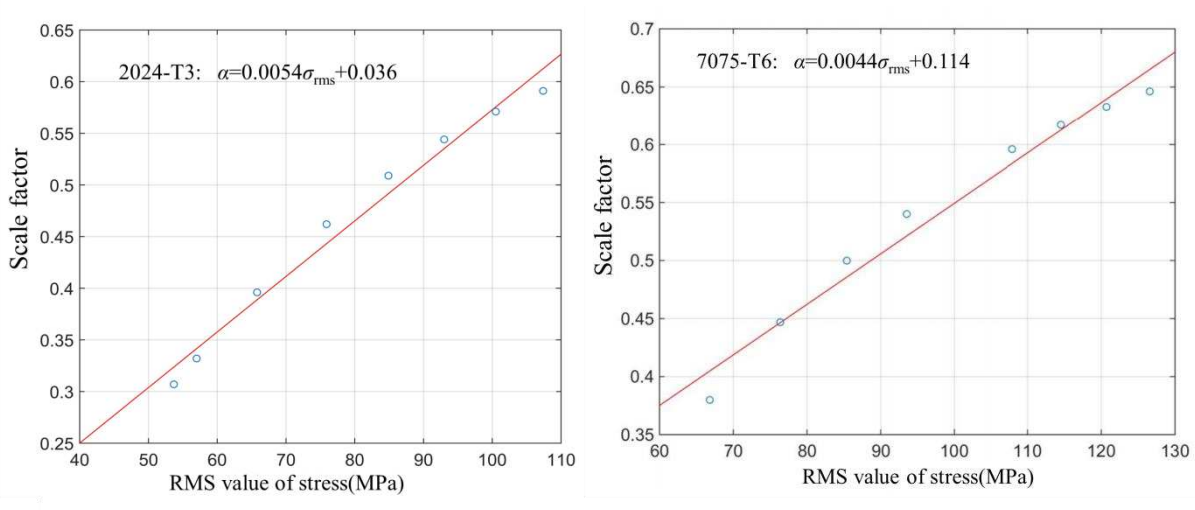

(a) 2024-T3 test specimen (b) 7075-T6 test specimen

Fig. 10. Scale factor.

Through the finite element analysis, the peak value of stress spectral density (see Fig. 8), the RMS value of stress σ_{rms} (see Fig. 9) and the scale factor (see Fig. 10) at the hot-spots were obtained so that the acceleration factor was calculated directly obtaining the results listed in Tab. 2.

Table 2

Scale factor and acceleration factor under different excitation spectrum.

Material	Acceleration spectrum	Peak of stress PSD ($MPa^2.Hz^{-1}$)	RMS value of stress (MPa)	Scale factor α	Acceleration factor γ
2024-T3	S1-0	3952.9	53.7	0.326	——
	S1-1	9882.9	84.9	0.494	5.27
	S1-2	11859.7	93.0	0.538	7.42
	S1-3	13836.5	100.5	0.579	9.95
7075-T6	S2-0	6058.0	66.1	0.405	——
	S2-1	18173.7	114.5	0.618	6.15
	S2-2	20193.2	120.7	0.645	7.40
	S2-3	22212.7	126.6	0.671	8.77

4. Experimental validation

Electric vibration equipment DC-300-3 was used to run several vibration tests, which included sinusoidal frequency sweep tests and random vibration fatigue tests. Vibration data processing system RC-2000 was used for the output of the spectral response curve of the sinusoidal frequency sweep, as shown in Fig 11 (where f_1, f_2 and f_3 are the first three natural frequencies). Then the random vibration load spectrum was loaded. The excitation signals of the electric vibration table were detected via acceleration sensor YMC2106C, which was mounted on the base of the vibration table. The response signal near the counterweight was gathered by another YMC2106C acceleration sensor. The edge of the elliptical hole in the

test specimens was monitored continuously during testing until cracks occurred.

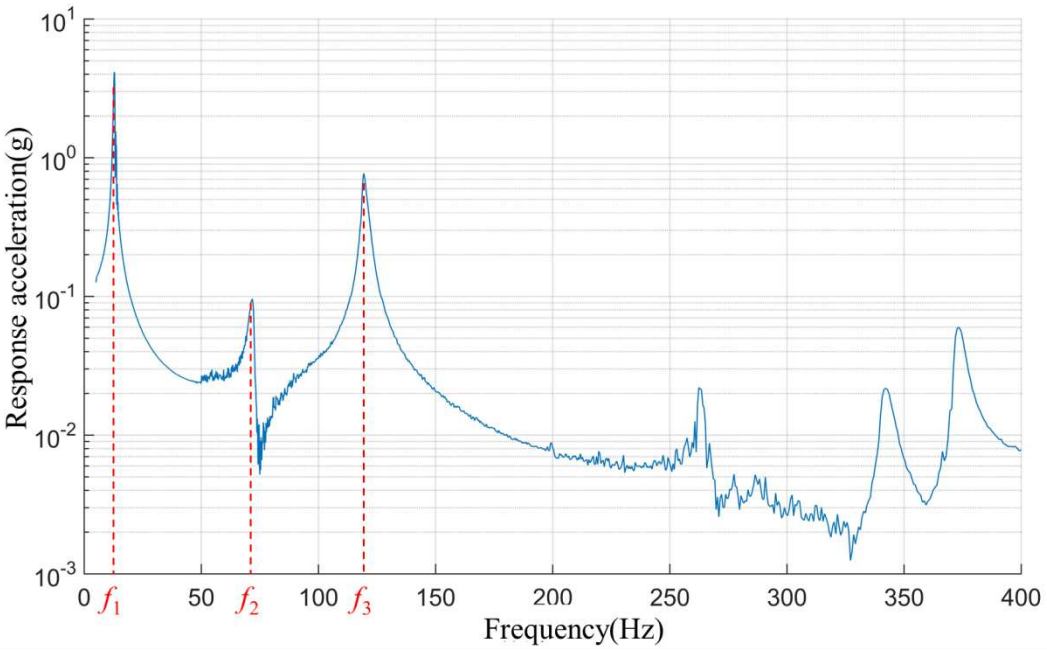

Fig. 11. Spectral response curve of sinusoidal frequency sweep.

Table 3 shows the vibration time corresponding to a 1mm crack at the edge of the elliptical hole. This was taken as the vibration fatigue crack initiation life of the test specimen.

Table 3

Results of vibration fatigue test.

Material	Acceleration spectrum	Vibration fatigue life(min)	Average lifetime(min)
2024-T3	S1-0	485.8、531.7、472.3、706.7	549.1
	S1-1	124.5、124.5、93.7、89.5、85.1、92.6	101.6
	S1-2	101.5、29.2、86.5、94.4、86.9、64.3	77.2
	S1-3	68.1、55.5、55.5、67.5、66.3、38.3	58.5
7075-T6	S2-0	972.7、1044.1、990.5、1199.7	1051.8
	S2-1	231.5、161.2、188.4、226.7、116.0、140.4	177.4
	$S2_I$-2	192.3、175.6、111.0、164.5、172.3、149.7	160.9
	S2-3	166.8、110.8、154.7、115.5、122.9、83.1	125.6

By taking S1-0 and S2-0 as the original spectrum and the other excitation spectrum as the acceleration spectrum, the test value γ of the vibration fatigue acceleration factor was calculated. The estimated value of the acceleration factor calculated in Table 2 is included in Table 4. As it can be seen from Table 4, the experimental value is in good agreement with the calculated value.

Table 4

Acceleration factor validation γ.

Material	Acceleration spectrum	Calculated value	Experimental value	Error(%)
2024-T6	S1-1	5.40	5.27	2.41
	S1-2	7.11	7.42	4.36
	S1-3	9.43	9.95	5.51
7075-T6	S2-1	5.93	6.15	3.71
	S2-2	6.54	7.40	13.15
	S2-3	8.37	8.77	4.78

5. Conclusions

(1) This paper proposes a calculation method of the acceleration factor, which is based on narrow-band random excitation and three-parameter S-N curve. This method is seen to have better accuracy than the traditional inverse power rate model.

(2) The concept of scale factor α was also proposed in this paper and the relationship between the obtained scale factor and the root mean square stress value σ_{rms} was seen to be approximately linear.

Declaration of Competing Interest

The authors declare that they have no known competing financial interests or personal relationships that could have appeared to influence the work reported in this paper.

References

[1] Z. Wang, B. Liu, L. Wang, The finite element verification of the non-gaussian acceleration random vibration theory method based on Grms-N, Chin. J. App.Mech. 37(6) (2020) 2386-2394.

[2] Li Q.Li, G. Cheng, H. Yao, Test method of vibration acceleration factor, J. Vib. Measurement Diag. 33(1) (2013) 35-39.

[3] G. Allegri, X. Zhang, On the inverse power laws for accelerated random fatigue testing, Int. J. Fatigue 30 (2008) 967-977.

[4] D. Benasciutti, Some analytical expressions to measure the accuracy of the “equivalent von Mises stress” in vibration multiaxial fatigue, J. Vib.Control 333 (2014) 4326-4340.

[5] Y. Jiang, J. Gun, Z. Li, et al, Experimental design and validation of an accelerated random vibration fatigue testing methodology, Shock Vib. (2015) 1-13

[6] Z.Wang, L.Wang, On accelerated random vibration testing of product based on component acceleration RMS-life curve, J. Vib. Control 24(15) (2018) 3384-3399.

[7] D. Shires, On the time compression (test acceleration) of broadband random vibration tests, Packag. Technol. Sci. 24(2) (2011) 75–87.

[8] C. Kim. Accelerated Sine-on-Random Vibration Test Method of Ground Vehicle Components over Conventional Single Mode Excitation. App.Sci. 7(8) (2017) 805.

[9] S. Ozsoy, M. Celik, and F.S. Kadioglu, An accelerated life test approach for aerospace structural components, Eng. Fail. Anal. 15(7) (2008) 946–957.

[10] A. Pothula, A. Gupta, G. R. Kathawate, Fatigue failure in random vibration and accelerated testing, J. Vib. Control 18(8) (2012) 1199–1206.

[11] X. Wu, C. Xie,K. Liu, et al , Study on high frequency vibration-induced fatigue failure of antenna beam in a metro bogie, Eng. Fail. Anal. 133(2022)

[12] W. Hu, Z. Liu,D. Liu,et al , Fatigue failure analysis of high speed train gearbox housings, Eng. Fail. Anal. 73 (2017) 57–71.

[13] K. Xu, Y. Wu, Q. Wu, Development of vibration loading profiles for accelerated durability tests of ground vehicles, Proceedings of the Dynamic Systems and Control Conference and Bath/ASME Symposium on Fluid Power and Motion Control (DSCC11) (2011) 717–724.

[14] M. Cesnik, J. Slavic, M.Boltezar, Uninterrupted and accelerated vibrational fatigue testing with simultaneous monitoring of the natural frequency and damping, J. Sound Vib. 331 (2012) 5370-5382.

[15] J.Wu , R.R.Zhang, Q.Wu, et al, Environmental vibration assessment and its applications in accelerated tests for medical devices, J. Sound Vib. 267 (2003) 371–383.

[16] C.R.Farrar, T.A.Duffey, P.J.Cornwell, et al, A review of methods for developing accelerated testing criteria, Proceedings of the 17th international modal analysis conference, Kissimmee, FL 17 (1999) 608–614.

[17] J. Klemenc, M. Fajdiga, An improvement to the methods for estimating the statistical dependencies of the parameters of random load states, Int. J. Fatigue 26 (2004) 141-154.

[18] N Santharaguru, S Abdullah, C. H.Chin, et al. Failure behaviour of strain and acceleration signals using various fatigue life models in time and frequency domains, Eng. Fail. Anal. 139 (2022)

[19] C. Lalanne, Random Vibration, National Defense Industry Press (2021).

[20] W.X. Yao, Structural fatigue life analysis, Science Press (2019). (in Chinese)

[21] R. Tovo, Cycle distribution and fatigue damage under broad-band random loading, Int. J. Fatigue 24 (2002) 1137-1147.

[22] Data sheet on mechanical properties of key Metal Materials for aircraft design.Beijing.Aviation Industry Press.2015. (in Chinese)